



Short communication

Ordered silicon nanocones as a highly efficient platinum catalyst support for direct methanol fuel cells

Jitendra N. Tiwari^a, Te-Ming Chen^a, Fu-Ming Pan^{a,*}, Kun-Lin Lin^b

^a Department of Materials Science and Engineering, National Chiao Tung University, Hsinchu 300, Taiwan, ROC

^b Department of Mechanical Engineering, National Taiwan University of Science and Technology, Taipei 0660, Taiwan, ROC

ARTICLE INFO

Article history:

Received 11 March 2008

Received in revised form 18 April 2008

Accepted 18 April 2008

Available online 3 May 2008

Keywords:

Silicon nanocone arrays

Pt catalysts

Mass activity

Methanol oxidation

ABSTRACT

Platinum nanoparticles were electrodeposited on ordered silicon nanocones (SNCs) and used as the catalyst for methanol electro-oxidation in direct methanol fuel cells (DMFCs). Because of uniform dispersion of Pt nanoparticles and the high surface area, the Pt-SNC electrode exhibited superior electrocatalytic properties toward the methanol electro-oxidation, with the onset potential of 0.08 V (vs. SCE). According to chronoamperometric analysis and CO stripping cyclic voltammetric (CV) study, the Pt/SNC electrode had a stable electro-oxidation activity with a very good CO tolerance. The Si surface oxide surrounding the Pt nanoparticles on the SNCs was suggested to play a key role in improving the CO tolerance via the bifunctional mechanism.

© 2008 Elsevier B.V. All rights reserved.

1. Introduction

In the past decade, extensive effort has been made to develop direct methanol fuel cells (DMFCs) for small portable electronic applications, such as the supplementary rechargeable battery for laptops and cellphones, etc. DMFCs fuel cell attracts such a wide attention is due to simple system design, low operation temperature, convenient fuel storage, high energy density and long life, as compared to conventional rechargeable power sources, such as Li ion batteries. Platinum and its alloys are normally used as the catalyst in DMFCs because of the high electrocatalytic activity for methanol oxidation. In order to increase the electrocatalytic mass activity and reduce usage of the precious Pt catalyst, most methods of fabricating Pt catalyst-supporting electrodes tried to disperse Pt nanoparticles on the electrode support so that creating a high catalytic surface area and reducing Pt consumption could be achieved together. Much effort was done to improve catalyst mass activity by different approaches, such as nanoporous graphite with Pt nanoparticles [1], carbon nanocoils with Pt–Ru catalyst alloys [2] and carbon-coated anatase TiO₂ nanocomposite [3]. However, many complications of using Pt catalyst nanoparticles for DMFCs still exist and need to be solved for better utilization of the Pt catalyst. In particular, CO poisoning effect and catalyst loss during

electrocatalytic reactions in DMFCs are among the major difficulties frequently addressed and widely studied.

In this report, Pt nanoparticles were electrodeposited on a highly ordered Si nanocone (SNC) array, which was fabricated by means of anodic aluminum oxide (AAO) templation method. The SNCs provided a high surface area for Pt catalyst loading, and the well ordered arrangement of the nanocones allowed a relatively uniform electric potential distribution over the nanocones during the Pt electrodeposition, thereby Pt nanoparticles could be well dispersed on the Si support and uniform in size. In addition, the SNCs were fabricated from a Si substrate of low resistivity, and thus the SNC support was very suitable for the use as the Pt electrocatalytic electrodes in respect of electrical conductivity. Moreover, the surface oxide formed on the SNC surface could enhance the CO tolerance of the Pt catalyst via bifunctional mechanism.

2. Experimental

The fabrication procedures of SNCs had been described elsewhere [4,5] and the experimental procedures are discussed in more detail in the supporting information and illustrated in Fig. S1. In brief, to fabricate silicon nanocones (SNCs), TiO₂ nanodots were first prepared on the Si wafer of low resistivity using AAO as the template. The TiO₂ nanodots were then used as the mask to regulate the arrangement of the highly ordered SNCs, which were produced by reactive-ion-etch (RIE). The desired dimension of the SNCs was controlled by the AAO preparation and RIE conditions, such as the

* Corresponding author. Tel.: +886 3 5131322; fax: +886 3 5724727.
E-mail address: fmpan@faculty.nctu.edu.tw (F.-M. Pan).

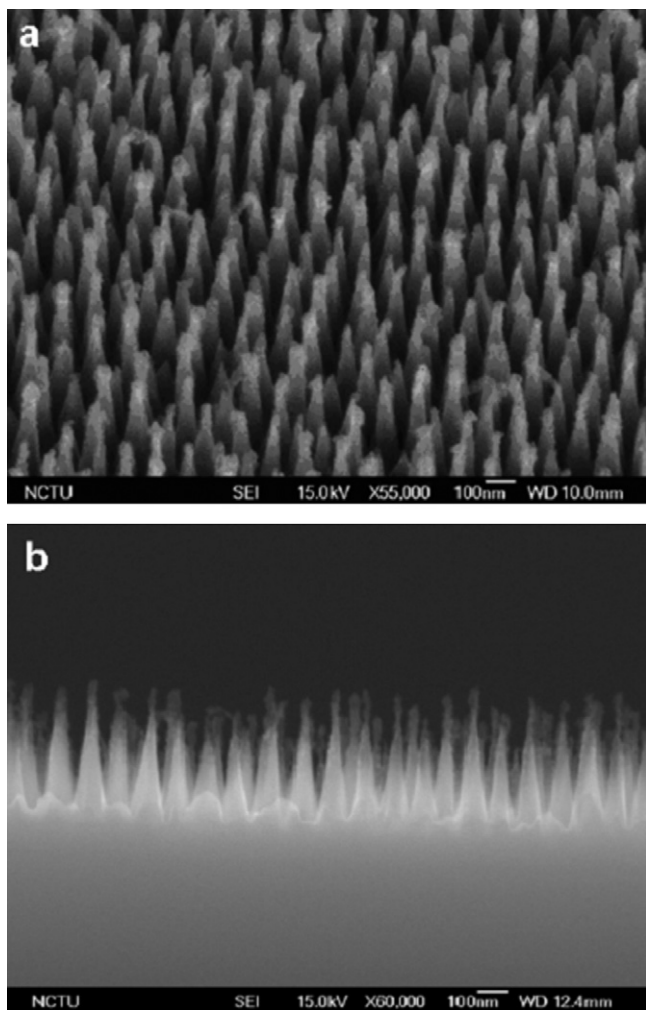


Fig. 1. SEM images of the ordered Si nanocones with electrodeposited Pt nanoparticles: (a) a side view, and (b) cross-sectional view.

Al anodization potential and the RIE plasma power. The Pt nanoparticles were electrodeposited on SNCs in an aqueous solution of 1 M K_2PtCl_6 /1 M HCl at 25 °C by potentiostatic pulse plating in a three-electrode cell. Bipolar pulses were used and the pulse height and duration were -0.09 mV and 7 ms for negative pulse, and $+0.02$ mV and 1 ms for the positive pulse, respectively. The positive potential pulse was applied to avoid particle coalescence so that nanosized Pt nanoparticles could be deposited on the Si nanocones. Chloride anions in the electrolyte solution tend to adsorb on Pt particles, making Pt nanoparticles better separated from each other due to electrostatic repulsion between negatively charged surface layers [6]. The size of Pt nanoparticles and mass loading of platinum on SNCs were controlled by the applied potential and pulse duration. The Pt/SNC electrode was rinsed thoroughly with deionized water to remove residual chlorine ions after Pt electrodeposition, and allowed to dry before use in the measurement cell. The CO adsorption on the Pt catalyst was performed by flowing the 10% CO/ N_2 gas mixture in the 1 M H_2SO_4 aqueous solution at 100 mV for 35 min. Before the CO stripping measurement, the solution was purged with N_2 gas for 30 min to removed CO remained in the solution.

3. Results and discussion

Fig. 1 shows the scanning electron microscopy (SEM, JEOL JSM-6700F) image of the SNC array with electrodeposited Pt

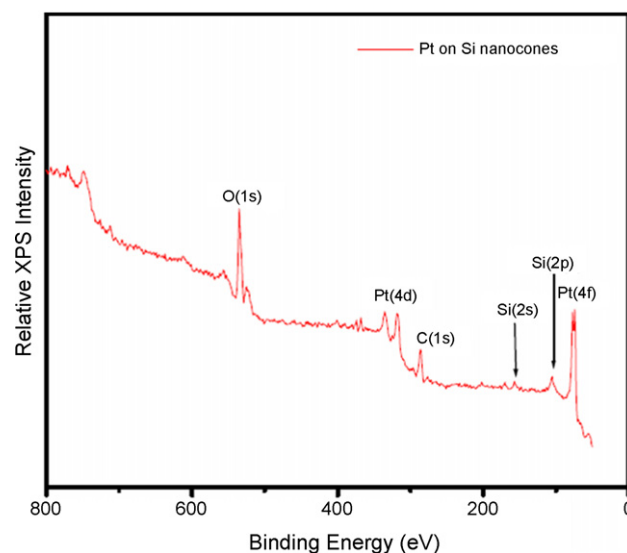


Fig. 2. X-ray photoelectron spectrum (XPS) of the Pt nanoparticles loaded SNC array, showing the presence of Pt on the nanocones.

nanoparticles. The well ordered SNCs, with a hexagonal arrangement, was ~ 300 nm high and had a base diameter of ~ 100 nm. X-ray photoelectron spectroscopy (XPS) shown in **Fig. 2** indicated the presence of Pt on the SNCs after the electrodeposition. According to the cross-sectional SEM image, Pt particles seemed to slightly accumulate on the tip of SNCs, but nanoparticles agglomeration on the sidewall of the nanocones was insignificant. Due to the very small size, Pt nanoparticles are hardly observed to adhere on the sidewall of the SNCs from the SEM images.

The Pt nanoparticles had a size smaller than ~ 5 nm according to transmission electron microscopy (TEM, JEOL JEM-3000F) study. **Fig. 3** shows the high resolution TEM image of a silicon nanocone with well dispersed Pt nanoparticles on it. The selected area

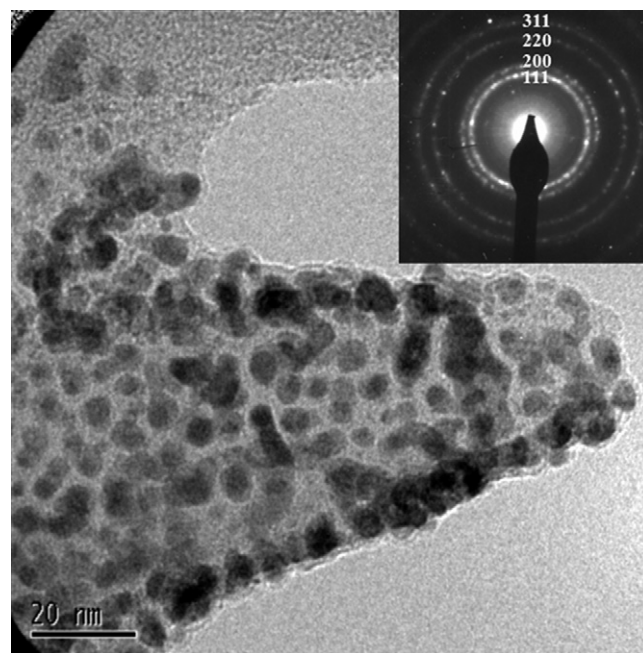


Fig. 3. High resolution TEM image of a Pt nanoparticles loaded Si nanocones. HRTEM image clearly shows that Pt nanoparticles are well dispersed on the Si nanocone. The inset is a selected area electron diffraction (SAED) pattern.

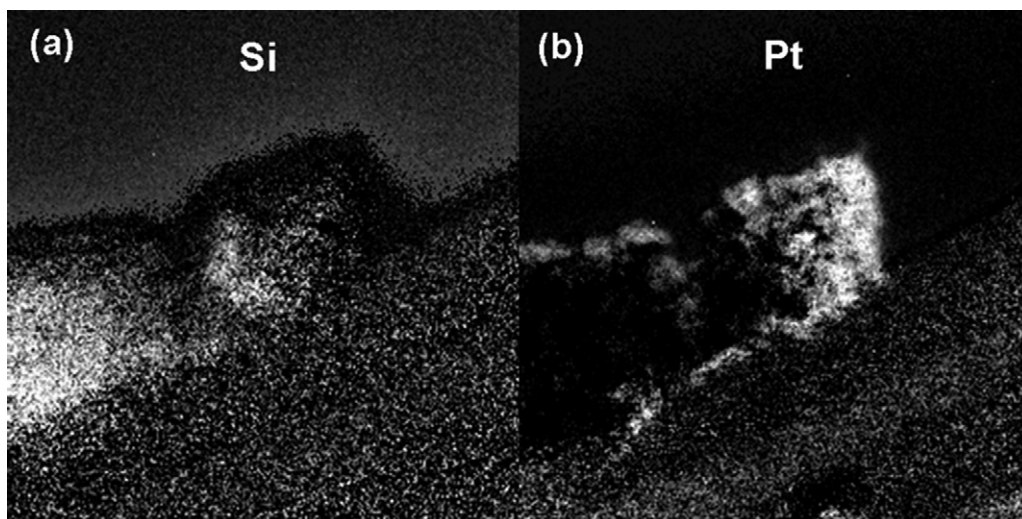


Fig. 4. EELS elemental mapping images of (a) Si and (b) Pt for the Pt nanoparticle loaded Si nanocones.

electron diffraction (SAED) pattern is shown in the inset of Fig. 3. Four diffraction rings can be indexed as (1 1 1), (1 1 0), (2 0 0) and (3 1 1) orientations for the Pt face center cubic (FCC) lattice structure. Electron energy loss spectroscopy (EELS) was also used to map the elemental distribution of Pt on the SNC, and the mapping shown in Fig. 4 clearly shows that Pt nanoparticles distributed on the tip and sidewall of the SNC.

The electroactive surface area (ESA) of the Pt loaded SNC electrode can be determined by CO stripping cyclic voltammetry. The CO stripping voltammogram for the Pt/SNC electrode in a CO saturated 1 M H₂SO₄ aqueous solution is shown in Fig. 5a. A high ESA of ~317 m² g⁻¹ was obtained for the Pt/SNC electrode by integrating the CO electro-oxidation peak area, assuming an oxidation charge of 420 μC cm⁻² for one monolayer of CO on a smooth Pt surface [7]. For comparison, the ESA of the Pt film electrodeposited on a flat Si substrate (hereafter abbreviated as Pt/Si) was calculated to be 38.9 m² g⁻¹ from Fig. 5b. The electrocatalytic stability of the Pt/SNC electrode was evaluated by repeating the cyclic voltammetric (CV) scan from -0.45 to 1.2 V in the 1 M H₂SO₄ solution for more than 1000 cycles. From Fig. 6, the CV curve of the 1000th cycle shows that the hydrogen adsorption/desorption peak had a peak current reduction by ~20% as compared with that of the second cycle, indicating possible Pt nanoparticle loss from the SNCs after 1000 cycles of hydrogen oxidation and reduction. Fig. 7 is the plots of the ESA as a function of the number of CV cycles for the Pt/SNC and the Pt/Si electrodes. The plots are normalized against the ESA of the first cycle. The ESA of the Pt/SNC electrode had a moderate drop for the first 100 CV cycles, and then progressively decreased to 75% of the initial ESA after 1000 CV cycles. On the other hand, the Pt/Si electrode shows a dramatic drop in the ESA in the first 200 cycles, followed by continuous and significant ESA decrease. The much smaller ESA loss of the Pt/SNC electrode suggests that the electrodeposited Pt nanoparticles were well adhered to the Si nanocones.

The Pt nanoparticles had a very high catalyst specific activity (current per ESA) for electro-oxidation of methanol. Fig. 8 shows the cyclic voltammogram of the Pt/SNC electrode in 1 M methanol/1 M H₂SO₄ aqueous solution. The unit of the y-axis of the CV plot is labeled by the current per ESA. The CV curve shows that the methanol oxidation peak had the maximum around 0.83 V vs. SCE and a very low onset potential of ~0.08 V. Also shown in Fig. 8 is the CV curve of the Pt/Si electrode, which shows a much smaller specific

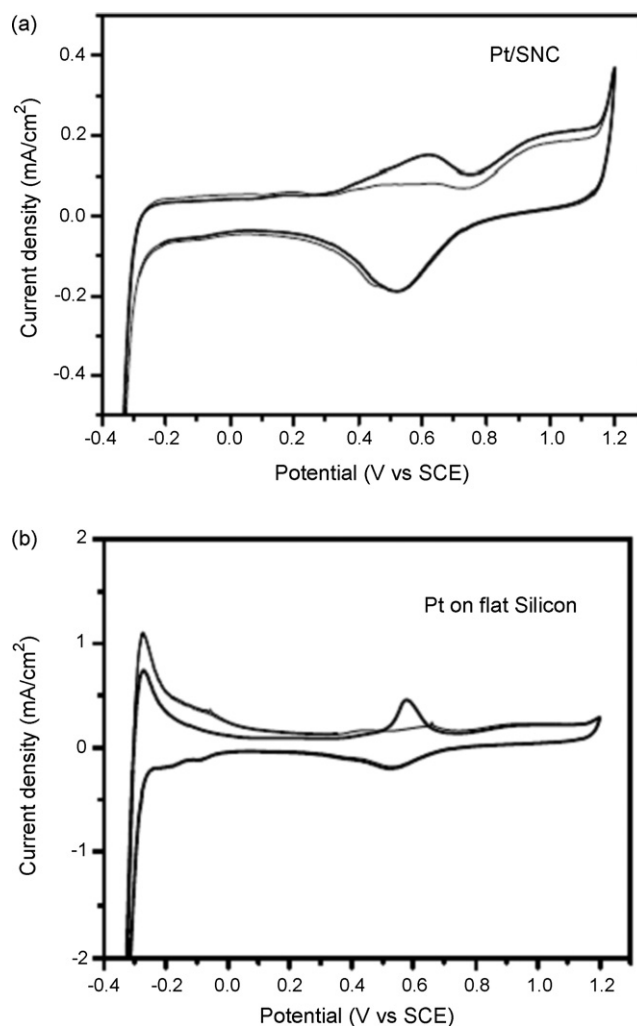


Fig. 5. CO stripping cyclic voltammograms of (a) Pt nanoparticles electrodeposited on the ordered SNCs and (b) the Pt film electrodeposited on the flat silicon substrate in a CO saturated 1 M H₂SO₄ solution. The scan rate is 20 mV s⁻¹.

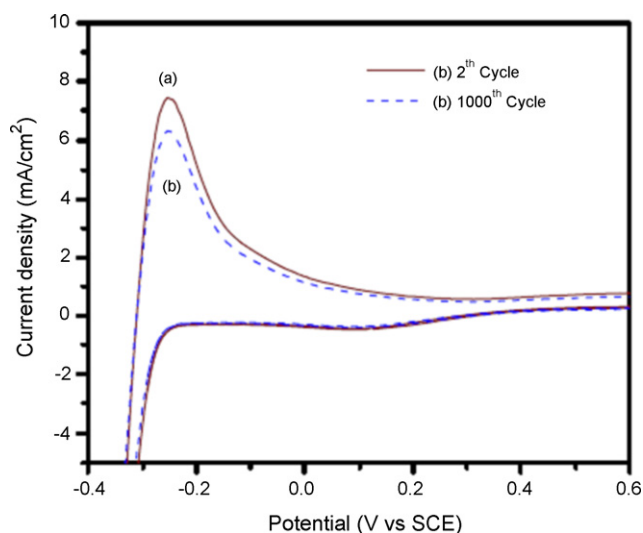


Fig. 6. Cyclic voltammograms for Pt/SNC electrode in 1 M H₂SO₄ aqueous solution at room temperature and with a scan rate of 25 mV s⁻¹: (a) the 2nd cycle and (b) the 1000th cycle.

activity with a high onset potential. The negative onset potential shifting indicated that the Pt nanoparticles on the ordered SNC array can effectively reduce overpotentials in the methanol electro-oxidation reaction [8–11]. Because of the very large ESA, the Pt/SNC electrode had a better electrocatalytic mass activity compared with many previously reported electrodes made from nanostructured materials. The mass activity of the Pt/SNC electrode at 0.4 V was ~ 0.53 A mg⁻¹ at room temperature, that was about six folds higher than that of the Pt loaded carbon nanocoils [2], and two folds higher than the carbon-coated anatase TiO₂ nanocomposite [3].

Fig. 9 shows the chronoamperogram of electroactivity of the Pt/SNC electrode at the oxidation potential ~ 0.3 V in the 1 M methanol/1 M H₂SO₄ aqueous solution at 25 °C. The chronoamperogram showed that electrocatalytic oxidation of methanol maintained a high activity and was very stable during the measurement for more than 2 h. The observation implied that most CO adspecies could be oxidized and removed from the Pt catalyst nanoparticles so that the catalytic oxidation of methanol could be kept proceeding efficiently on the Pt/SNC electrode. The argument was supported by the CO stripping cyclic voltammetry study. In

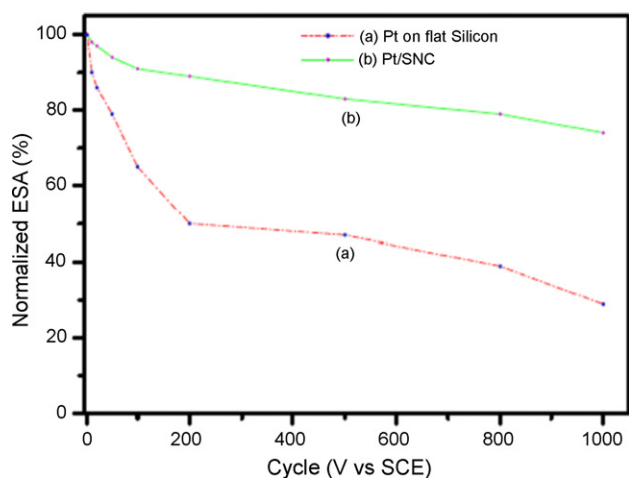


Fig. 7. The plot of electroactive surface area (ESA) as a function of the number of the cyclic voltammetric scan for (a) the Pt film electrode deposited on the flat Si substrate and (b) the ordered Pt/SNC electrode.

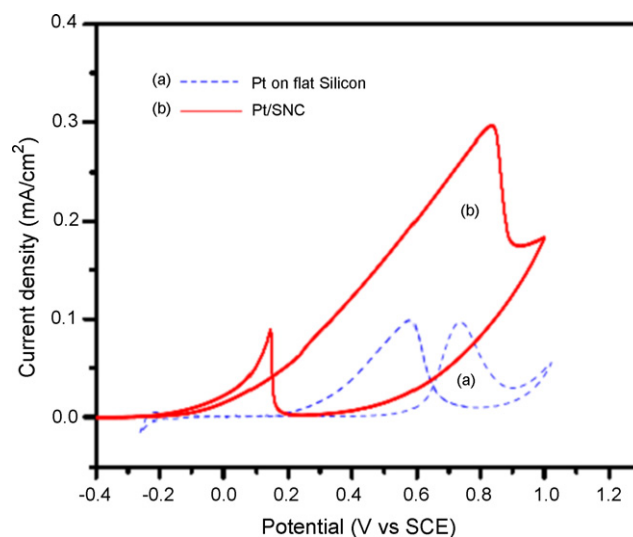


Fig. 8. Cyclic voltammograms of (a) the Pt film electrode deposited on the flat silicon substrate and (b) the Pt catalyst nanoparticles on the ordered SNC array in an argon saturated 1 M CH₃OH/1 M H₂SO₄ aqueous solution. The scan rate is 25 mV s⁻¹.

Fig. 5, the CO stripping voltammogram of the Pt-SNC electrode was compared with that of the Pt/Si electrode. For the Pt/SNC electrode, the onset of electro-oxidation of CO took place below ~ 0.3 V vs. SCE and the peak potential was ~ 0.6 V. On the other hand, the Pt/Si electrode had an onset potential for CO electro-oxidation ~ 0.5 V vs. SCE. The observation that the Pt/SNC electrode had a much lower onset potential in the CO stripping voltammogram indicated that electro-oxidation reaction of CO adspecies on Pt sites could be efficiently performed on the Pt/SNC electrode.

The excellent electrocatalytic performance of the Pt-SNC electrode can be explained as follows. First, the SNCs provided a large surface area for Pt nanoparticles loading, resulting in a very high catalytic mass activity. With the present nanocone geometry, the SNCs provided a surface area applicable for Pt loading six times (the ratio of the cone surface area to the cone base area) larger than a flat Si surface, and thus increased the mass activity accordingly. Second, nanosized and highly dispersed Pt catalyst nanoparticles

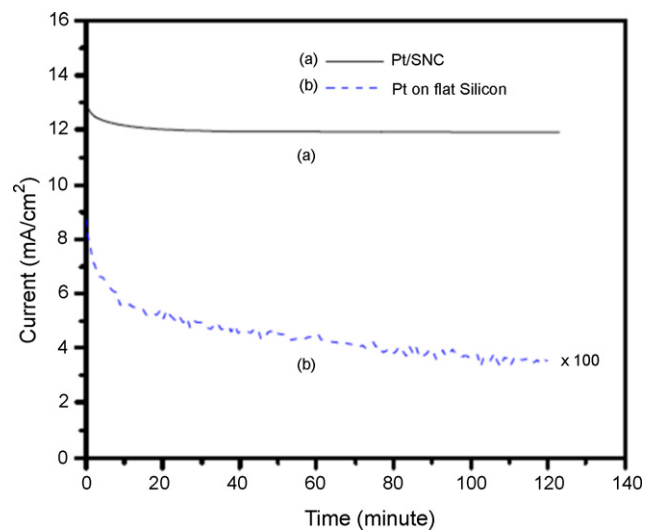


Fig. 9. The chronoamperometric response of (a) Pt nanoparticles electrodeposited on the ordered SNCs, and (b) the Pt film electrode deposited on the flat Si substrate in a saturated 1 M CH₃OH/1 M H₂SO₄ aqueous solution at 0.3 V (SCE) for 2 h. The scale of curve b is multiplies by 100.

were deposited on the SNCs. Unlike many reported porous electrodes, which had a very large surface area as well, the ordered SNCs may provide better electrodeposition conditions for well dispersed Pt nanoparticles. Because the arrangement of the SNCs was highly ordered, the potential distribution over the SNC array should be even and, therefore, the deposited Pt particles were uniform in size. Besides, compared with many porous supports, the SNC array had a larger open volume, allowing ionic species to diffuse more freely between Si nanocones, and thus Pt particles could be readily electrodeposited on the SNCs without significant agglomeration. By carefully tuning the pulse voltage and pulse duration, we can limit the Pt particle size to the nanometer range and mitigate particle coalescence, thereby increasing the electroactive area. Third, silicon oxide grown on the Si nanocones can play an important role in enhancing CO tolerance of the electrode via the bifunctional mechanism [12]. A nature SiO₂ layer is usually terminated with silanol groups. The bifunctional model describes that hydroxyl surface groups are able to oxidize and remove adjacent CO adspecies from the Pt catalyst surface, thus avoiding CO poisoning. Because the Pt nanoparticles were well dispersed on the SNCs, CO adspecies bound on the periphery of Pt nanoparticles can be readily oxidized by surrounding silanol groups. Moreover, due to the nanoscaled size of Pt catalyst, OH adspecies can migrate over the Pt nanoparticle without much difficulty and react with adsorbed CO via a Langmuir–Hinshelwood type reaction mechanism, in which adsorbed reactants diffuse, collide and form products on the surface, thereby facilitating a better efficiency of CO oxidation.

4. Conclusions

We have electrodeposited Pt catalyst nanoparticles on highly ordered SNCs fabricated by AAO templation method, and electrocatalytic oxidation of methanol on the Pt/SNC electrode was studied. Because of the large surface area of the Si nanocones and the highly dispersed nanosized Pt catalyst particles, the Pt/SCN electrode demonstrated a very high mass activity and a very low

onset potential. CV measurements, CO stripping cyclic voltammogram and chronoamperometric study indicated that the Pt nanoparticles were well adhered to the Si nanocones and the Pt/SNC electrode had a very good CO tolerance. We ascribed the good CO tolerance to the efficient CO oxidation by the abundant silanol groups surrounding the Pt nanoparticles via bifunctional mechanism.

Acknowledgements

This work was supported by the National Science Council of R.O.C., under Contract no. NSC93-2120-M-009-007. Technical support from the National Nano Device Laboratories (NDL) is gratefully acknowledged.

Appendix A. Supplementary data

Supplementary data associated with this article can be found, in the online version, at [doi:10.1016/j.jpowsour.2008.04.058](https://doi.org/10.1016/j.jpowsour.2008.04.058).

References

- [1] S.H. Joo, S.J. Choi, I. Oh, J. Kwak, Z. Liu, O. Terasaki, R. Ryoo, *Nature* 412 (2001) 169.
- [2] T. Hyeon, S. Han, Y.-E. Sung, K.W. Park, Y.W. Kim, *Angew. Chem. Int. Ed.* 42 (2003) 4352.
- [3] S. Shanmugam, A. Gedanken, *Small* 3 (2007) 1189.
- [4] P.L. Chen, C.T. Kuo, T.G. Tsai, B.W. Wu, C.C. Hsu, F.M. Pan, *Appl. Phys. Lett.* 82 (2003) 2796.
- [5] T.M. Chen, F.M. Pan, J.Y. Hung, L. Chang, S.C. Wu, C.F. Chen, *J. Electrochem. Soc.* 154 (2007) D215.
- [6] I. Lee, K.-Y. Chan, D.L. Phillips, *Appl. Surf. Sci.* 136 (1998) 321.
- [7] J.W. Kuo, T.S. Zhao, J. Prabhuram, R. Chen, C.W. Wong, *Electrochim. Acta* 51 (2005) 754.
- [8] C.T. Hable, M.S. Wrighton, *Langmuir* 7 (1991) 1305.
- [9] M.J. Gonzalez, C.T. Hable, M.S. Wrighton, *J. Phys. Chem. B* 102 (1998) 9881.
- [10] M.J. Gonzalez, C.H. Peters, M.S. Wrighton, *J. Phys. Chem. B* 105 (2001) 5470.
- [11] C.T. Hable, M.S. Wrighton, *Langmuir* 9 (1993) 3284.
- [12] B. Liu, J.H. Chen, X.X. Zhong, K.Z. Cui, H.H. Zhou, Y.F. Kuang, *J. Colloid Interface Sci.* 307 (2007) 139.